



ALMA MATER STUDIORUM
UNIVERSITÀ DI BOLOGNA

ARCHIVIO ISTITUZIONALE DELLA RICERCA

Alma Mater Studiorum Università di Bologna Archivio istituzionale della ricerca

A computer vision approach based on deep learning for the detection of dairy cows in 2 free stall barn

This is the final peer-reviewed author's accepted manuscript (postprint) of the following publication:

Published Version:

Tassinari, P., Bovo, M., Benni, S., Franzoni, S., Poggi, M., Mammi, L.M.E., et al. (2021). A computer vision approach based on deep learning for the detection of dairy cows in 2 free stall barn. COMPUTERS AND ELECTRONICS IN AGRICULTURE, 182, 1-15 [10.1016/j.compag.2021.106030].

Availability:

This version is available at: <https://hdl.handle.net/11585/800275> since: 2021-02-16

Published:

DOI: <http://doi.org/10.1016/j.compag.2021.106030>

Terms of use:

Some rights reserved. The terms and conditions for the reuse of this version of the manuscript are specified in the publishing policy. For all terms of use and more information see the publisher's website.

This item was downloaded from IRIS Università di Bologna (<https://cris.unibo.it/>).
When citing, please refer to the published version.

(Article begins on next page)

1 A computer vision approach based on deep learning for the detection of dairy cows in 2 free stall barn

3 Patrizia Tassinari^a, Marco Bovo^a*, Stefano Benni^a, Simone Franzoni^b, Matteo Poggi^b, Ludovica Maria Eugenia
4 Mammi^c, Stefano Mattoccia^b, Luigi Di Stefano^b, Filippo Bonora^a, Alberto Barbaresi^a, Enrica Santolini^a, Daniele
5 Torreggiani^a

6 ^a Department of Agricultural and Food Sciences, University of Bologna, Bologna, Italy

7 ^b Department of Computer Science and Engineering, University of Bologna, Bologna, Italy

8 ^c Department of Veterinary Medical Sciences, University of Bologna, Bologna, Italy

9 * **Corresponding author.** Email: marco.bovo@unibo.it

10 Abstract

11 Precision Livestock Farming relies on several technological approaches to acquire in the most efficient way
12 precise and up-to-date data concerning individual animals. In dairy farming, particular attention is paid to the
13 automatic cow detection and tracking, as such information is closely related to animal welfare and thus to
14 possible health issues. Computer vision represents a suitable and promising method for this purpose.

15 This paper describes the first step for the development of a computer vision system, based on deep learning,
16 aiming to recognize in real-time the individual cows, detect their positions, actions and movements and record
17 the time history outputs for each animal.

18 Specifically, a neural network based on deep learning techniques has been trained and validated on a case
19 study farm, for the automatic recognition of individual cows in videos recorded in the barn. Four cows were
20 selected to train and validate a YOLO neural network able to recognize a cow starting from the coat pattern.
21 Then, precision-recall curves of the identification of individual cows were elaborated for both the specific
22 target classes and the whole dataset in order to assess the performances of the network.

23 By means of data augmentation techniques, an enlarged dataset has been created and considered in order to
24 improve the performance of the network and to provide indications to increase detection efficiency in those
25 cases where data acquisition is not easy to be carried out for long periods. The mean average precision of the
26 detection, ranging from 0.64 to 0.66, showed that it is possible to properly identify individual cows based on
27 their morphological appearance and that the piebald spotting pattern of a cow's coat represents a clearly
28 distinguishable object for a computer vision network. The results also led to obtain indications about the
29 quantity and the characteristics of the images to be used for the network training in order to achieve efficient
30 detections when facing with applications involving animals.

31

32 **Keywords:** precision livestock farming; computer vision; deep learning; dairy cow; herd management

33

List of symbols

Symbol	Description
A_t	Average Area of the bounding boxes in training phase
A_v	Average Area of the bounding boxes in validation phase
O_t	number of Occurrences in training phase
O_v	number of Occurrences in validation phase
tp	true positive
tn	true negative
fp	false positive
fn	false negative
P	Precision
R	Recall
F_1	F_1 -score
Pr	detection Probability
C	Confidence score
AP	Average Precision
mAP	mean Average Precision
IoU	Intersection over Union
AIoU	Average Intersection over Union

35

36

37 **1. Introduction**

38 The implementation of precision livestock farming (PLF) techniques in animal husbandry involves many fields
39 of the technological innovation and several researchers are currently seeking to apply new methodologies and
40 algorithms for both commercial and research purposes (Tullo et al., 2019). In particular, with reference to
41 innovative applications in the livestock sector, the animals are increasingly being analyzed and studied with
42 the help of informatics tools such as support vector machines, random forests techniques, neural networks,
43 machine learning approaches etc. (Kamilaris and Prenafeta-Boldú, 2018; Tsai and Huang, 2014; Li et al., 2017;
44 Okura et al., 2019). In this context, multiple challenges involve the dairy cattle sector, where the methods
45 currently available are often unsuitable to manage the collected data and to fully extrapolate the potential
46 informative content.

47 In fact, weather stations monitoring barn temperature and humidity, robotic milking systems helping the daily
48 work of the farmers, collars and pedometers controlling animals' activities and positions (Berckmans, 2014)
49 are capable to collect huge amounts of real-time data currently used to support the herd management.

50 PLF has thus contributed to switch the analysis framework of a farm from a data-poor to a data-rich situation:
51 the research key challenge is actually to turn those data into knowledge able to provide decision-maker with
52 real-time support for the cattle farm optimization (Barkema et al., 2015; Bewley et al., 2017; Fournel et al.,
53 2017; Van Hertem et al., 2014; Halachmi et al., 2013; Guzhva et al., 2016; Martinez-Ortiz et al., 2013).

54 Several researches have pointed out the opportunity to develop both algorithms suitable to provide early
55 warning and control systems able to optimize animal welfare and productivity based on data collected through
56 Information Communication Technology (ICT) systems (Alsaad et al., 2019; Jaeger et al., 2019; Cowley et al.,
57 2015). In this context, computer vision together with numerical analysis methodologies proved to have
58 fundamental importance (Van Hertem et al., 2018) . Computer Vision techniques are meant to be applied in
59 this research field in order to automate actions normally carried out by the human visual system (Taigman et
60 al., 2014). The aim of these algorithms is to “teach” a computer to apprehend from images and videos in order
61 to simulate the human vision and substitute the human beings in repetitive or complex actions. They have
62 already been tested on animals with promising results (Norouzzadeh et al., 2017; Trnovszky et al., 2017), also
63 in the livestock farming area (Aydin, 2017; Van Hertem et al., 2013), but recognizing each individual cow within
64 the herd is still representing a challenging issue.

65 The monitoring of position and movements of the individual animals may be necessary to quantify the main
66 indices related to animal welfare (Song et al., 2008; Jiang et al., 2019) and behavior (Porto et al., 2013, 2015),
67 as well as to identify any preferences of the cows regarding different zones of the barn.

68 Moreover, video monitoring of the herd, together with the adoption of quantitative criteria to control animal
69 welfare by means of computer vision, may represent a tool to improve citizens’ consciousness about rearing
70 conditions and increase their knowledge about feeding and housing practices. A recent study found that fresh
71 food and water, pasture access, gentle handling, space, shelter, hygiene, fresh air and sunshine, social
72 companions, absence of stress, health and safety from predators are considered by citizens as necessary
73 requirement for dairy cattle “good life” (Ventura et al., 2016). These results suggested that a transparent
74 exposure of livestock farming to the public may resolve some concerns, and video recording appear to be a
75 powerful tool for an effective and widespread information.

76 Therefore, the monitoring requirements can be considered according to two main levels of information and
77 complexity. The first one concerns the identification at regular time intervals of the number of animals that
78 are in a certain position, for example lying in a cubicle, standing at the manger etc. The second one deals with
79 the identification, instant by instant, of the behavior of the individual cows, with the possibility of calculating,
80 for each animal, the time spent in each position and the temporal sequence of its positions, including the
81 trajectory of its movements.

82 The first level of information makes it possible to quantify the aforementioned indices and to have an overview
83 of the performances of the general animal welfare conditions in the farm, by appropriately integrating these
84 indices with information on feeding and productivity of the animals, which can be deduced from other sources,
85 such as the milking robots and mixed ration delivery systems. The second level of information allows to have
86 specific information on the individual cow welfare condition and on the use of the various areas of the barn
87 and represents a challenge for innovation in PLF. A computer vision system implemented through deep
88 learning constitutes a suitable approach to achieve the latter objective.

89 The aim of this study is to develop and test the reliability level of a computer vision system, based on deep
90 learning techniques, for the automatic recognition of individual cows within images representing their
91 position. In particular, whilst developing a new software framework lies outside the scope of this paper, the
92 paper focuses on methodological aspects related to a more efficient application of ICT in the dairy cows
93 monitoring field. In fact, while object detection is already applied in commercial applications in various
94 contexts, individual cow recognition still represents an open issue for both the research and commercial fields,
95 since no consolidated approach still exists. Actually, some of these blocks of information are collected by
96 means of different very expensive sensors (ALLFLEX, 2020; DELAVAL, 2020; AFIMILK, 2020), the most of them
97 to be worn by the animals but with the system proposed here, it will be possible to collect wider information,
98 with a less expensive technology and finally yet importantly using a system that avoids the problems and labor
99 due to wearable sensors.

100 Therefore, the paper focuses on the selection, validation and performance assessment of a neural network, in
101 terms of speed and accuracy, and at the same time outlines the key issues of the broader process, which is

102 strictly depending and related to the enabling steps presented in the paper. Further testing and validating cow
103 detection procedures in various contexts, in different types of livestock structures, and in different operating
104 conditions, is an important research field, contributing to the definition of consolidated approaches enabling
105 cow recognition, displacement tracking and cow action/behavior (eating, drinking, lying down, standing etc.)
106 recognition systems. This system could represent an innovative and useful tool to support the farmer in the
107 daily management and decision-making. In fact, by means of the technology proposed here, it will be possible
108 to calculate, for example, the indices connected to animal welfare but also to check the time spent for
109 nutrition, drinking and walking. The outcomes of this monitoring could be effectively used by the farmers to
110 identify potential anomalies or diseases and promptly apply specific corrective actions (e.g. on the fans
111 controlling the barn environmental conditions, water supply, etc.). In addition to the technological system and
112 the experimental setup adopted, the paper describes an innovative algorithm for the detection of the cows
113 implemented and tested on a case study farm with computer vision procedures. The promising results
114 reported here represents a first preliminary contribution to the progress of the computer vision for herd
115 monitoring applications and could be an important support for the following study of the movements of the
116 cows in the barn and for the analysis of their actions and behavior.

117

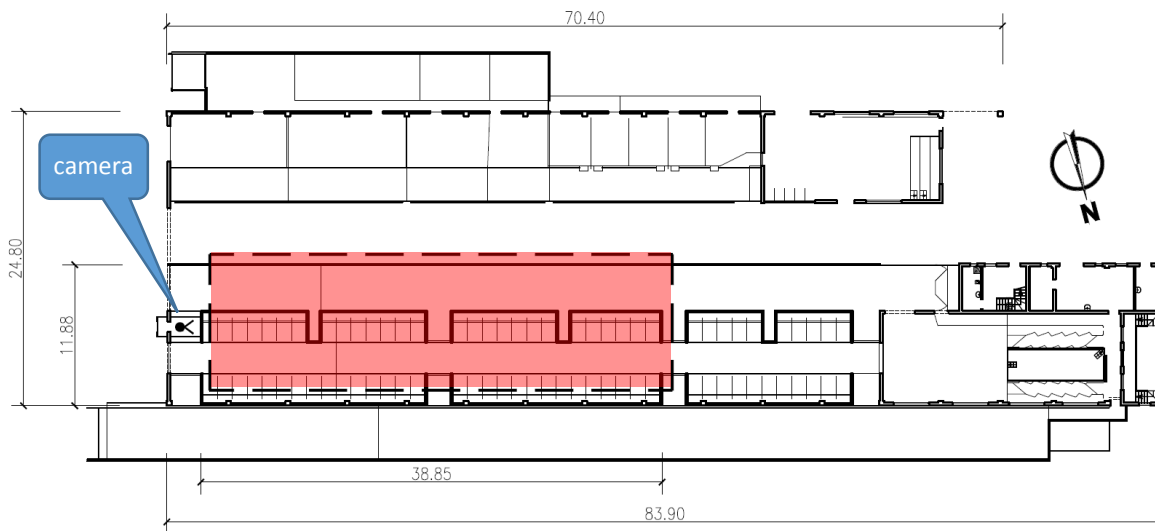
118 2. **Materials and methods**

119

120 2.1 *Study case*

121 The case study considered in this work is the experimental dairy cattle farm of the University of Bologna,
122 located in Ozzano Emilia, Bologna, in the North-East of Italy, where Holstein Friesian cattle is reared. This farm
123 is managed by the Department of Veterinary Medical Science and represents a unique reality in the national
124 context, thanks to its equipment and monitoring systems, which will allow to carry out the integrated analyses
125 aimed at the definition of models for the interpretation of milk production, reproductive, environmental and
126 management data. The building is a free stall experimental barn hosting about 150 animals, including 80 cows
127 (72 milking and 8 dry cows, and 70 among calves and heifers). The barn has a resting area in bedding material
128 for dry cows and litter cubicles for lactating cows (see Figure 1). A layout of the building is showed in Figure 1.

129 The barn is provided with cooling ventilation systems based on the Temperature-Humidity Index (THI) value.
130 The cows are milked twice a day and for each cow, the behavioral, productive and health parameters are daily
131 recorded automatically. The animals are fed with total mixed ration and auto-feeders for concentrate
132 supplementation.
133



134 Figure 1. Layout of the experimental barn. The dashed line delimitates the area framed by the camera (red
135 colored).
136
137

138 2.2 Software and neural network

139 2.2.1 Tagging software

140 VoTT (Visual object Tagging Tool) (Microsoft, 2018) was the software selected for the tagging tasks. It is an
141 open source annotation and labelling tool for image and video assets, it is a React + Redux Web application
142 written in Typescript. This software has been selected because it has several features, useful for the application
143 in the field of the present work. For example, it has an extensible model for importing data from local or cloud
144 storage providers and an extensible model for exporting labelled data to local or cloud storage providers.
145 Moreover, it has been developed not only to analyze images, but also video frames. So, it is possible to decide
146 the interval of frames per second and VoTT automatically transforms a video in a set of pictures. VoTT was
147 programmed following the 'Bring Your Own Data' (BYOD) approach and in VoTT, connections are used to
148 configure and manage source, i.e. the assets to label, and the target, i.e. the location to which labels should
149 be exported. Then, for the development of the computer vision technology in the field of animal monitoring,

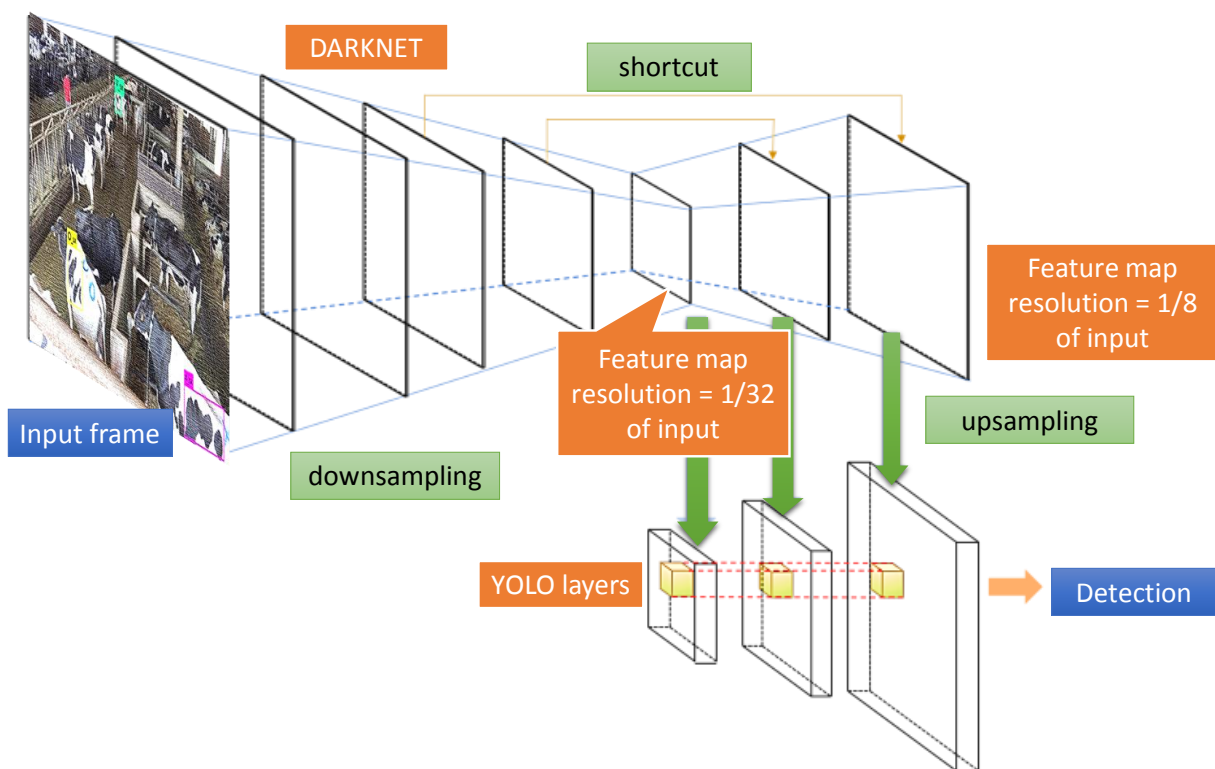
150 VoTT results very practical to set up and facilitate an end-to-end machine learning pipeline. In this work the
151 version 1.0.8 has been used.

152

153 2.2.2 *Detection algorithm and deep learning network*

154 At the state-of-the-art, in the field of computer vision for object detection, different more or less efficient
155 algorithms could be considered. For example, region-based convolutional neural networks (R-CNNs) (Girshick
156 et al., 2014) have been a pioneering approach that applies deep models to object detection. Actually, Faster
157 R-CNN (Ren et al., 2017) has been proved to be one of the most performing of its class, if compared with R-
158 CNN and Fast R-CNN (Girshick, 2015) and it has been already applied for cow detection for instance by (Bezen
159 et al., 2020). Different is the approach implemented in YOLO - You Only Look Once (Redmon et al., 2016),
160 where predictions are made with a single network evaluation, thus making the process much faster than
161 region-based convolutional neural networks (R-CNN) which require thousands of evaluations for a single
162 image. YOLO presents a totally different approach from prior detection systems, which proposes classifiers or
163 localizers to perform detection. It is one of the state-of-the-art detectors which are capable of localizing and
164 classifying multiple objects in images. In particular, the detector is faster than two-stage detectors: while they
165 propose object regions first and investigate the regions for object localization and classification, YOLO
166 combines the two stages into one neural network. Therefore, instead of applying the model to an image at
167 multiple locations and scales, so that high-score regions of the image are considered detections, Yolo applies
168 a single neural network to the full image. This network divides the image into regions and predicts bounding
169 boxes and probabilities for each region and these bounding boxes are weighted by the predicted probabilities.
170 The improvements in YOLO v3 (Redmon and Farhadi, 2018) made the algorithm even faster and suitable for
171 problems like those investigated here. In fact, the future real applications of this system will face with the
172 detection of large number of cows in a herd, during the time, and should be able to recognize the possible
173 action the cow is doing in real-time. For this reason a fast algorithm is necessary and this has driven the choice
174 of the authors towards the framework Darknet (Redmon, 2013), an open source framework for neural network
175 development including YOLO v3. The algorithm has the advantage to look at the whole image at test time, so

176 that predictions are informed by the global context of the image (see Figure 2). More specifically, YOLO v3
177 predicts an objectness score for each bounding box using logistic regression. This score should be 1 if the
178 bounding box prior overlaps a ground truth object by more than any other bounding box prior. Each box
179 predicts the classes the bounding box may contain using multi-label classification. At the current state of the
180 research the authors selected and adopted YOLO v3 as detection system but the evaluation of the
181 performances of different detection algorithms, for the problem investigated here, will be object of future
182 investigations.
183



184
185 Figure 2. Architecture of YOLO v3.

186
187 **2.3 Data collection**

188 As the performance of the neural network are strictly connected to the quantity and the quality of the training
189 dataset, particular attention was paid to the collection of a suitable dataset of video frames. The videos were
190 registered by a HDR-CX115E (Sony) camera (see Figure 3) in a high quality standard (HD resolution, 25 frames

191 per second). The recording has been conducted on a tripod positioned 2 meters above the barn floor, so the
192 total height for the recording was about 3.50 meters.
193 The section recorded by the camera focused on the feeding area, including the rack (on the left) and the
194 cubicles (on the center and on the right of the frames). A limitation of this position is that the images of the
195 cows up in the trough are greater for quality and quantity, so the dataset is composed by more photos of the
196 left hips than the right ones.



197

198 Figure 3. The HDR-CX115E camera positioned for video recording.

199

200 **2.4 Research method**

201 The research has been structured in the following main phases:

- 202 1) random selection in the herd of a sample of 10% of the cows' population in the free stall area monitored
203 by the camera (i.e. about 40 cows) during the recording phase. The sample is suitable to verify if the
204 network is capable to recognize a cow among others and to distinguish between more animals. Then the
205 animals have been marked, with a specific blue paint, with a letter only to help the identification of the
206 cows in the different frames. It is worth to notice this aspect since the neural network has not been

- 207 trained based on these symbols but the bounding boxes considered only pelt portions with natural
208 pattern of the cows;
- 209 2) recording of the videos after selecting the more suitable position for the camera;
 - 210 3) creation of the dataset for the training phase;
 - 211 4) training of the neural network, i.e. definition of the parametric weights for object recognition;
 - 212 5) validation test of the neural network with the weights defined in phase 4 and scoring the results by means
213 of the performance indicators defined before;
 - 214 6) creation of an augmented “virtual” dataset aiming to improve the detection performances of the network
215 for the classes poorly represented in the frames used for the network training;
 - 216 7) repetition of the phases from 3 to 5 in order to assess the improvement in the detection performances
217 after the manipulations operated to the frame dataset.

218

219 **2.5 Experimental setup and tests**

220 Four cows have been selected to train and test the neural network adopted in the study. The four letters X, V
221 O and I have been used only to identify a specific cow and the letter corresponding to each cow was drawn on
222 both right and left hips and on the forehead of the various cows. Two types of classes have been defined for
223 the identification of each cow corresponding to the pelt of the hips of the four cows. A total number of 8
224 classes (4 cows × 2 hips) has been adopted for the neural network training/validation in order to recognize the
225 cows by the black-white pattern of each specific pelt. Therefore, each class was identified by the capital letter
226 indicating the cow followed by right (r) or left (l) for identify the two different hips. The eight classes considered
227 in the study are: X_{left} , X_{right} , V_{left} , V_{right} , O_{left} , O_{right} , I_{left} and I_{right} . For example, Figure 4 illustrates the internal view
228 of the barn with a detail of the blue paint on the right hip of the cow labelled “V”, thus labelled as class V_{right} .



229

230 Figure 4. Example of a frame with detail of the blue paint on the right hip of the cow labelled “V” so
231 representing the class V_{right} .

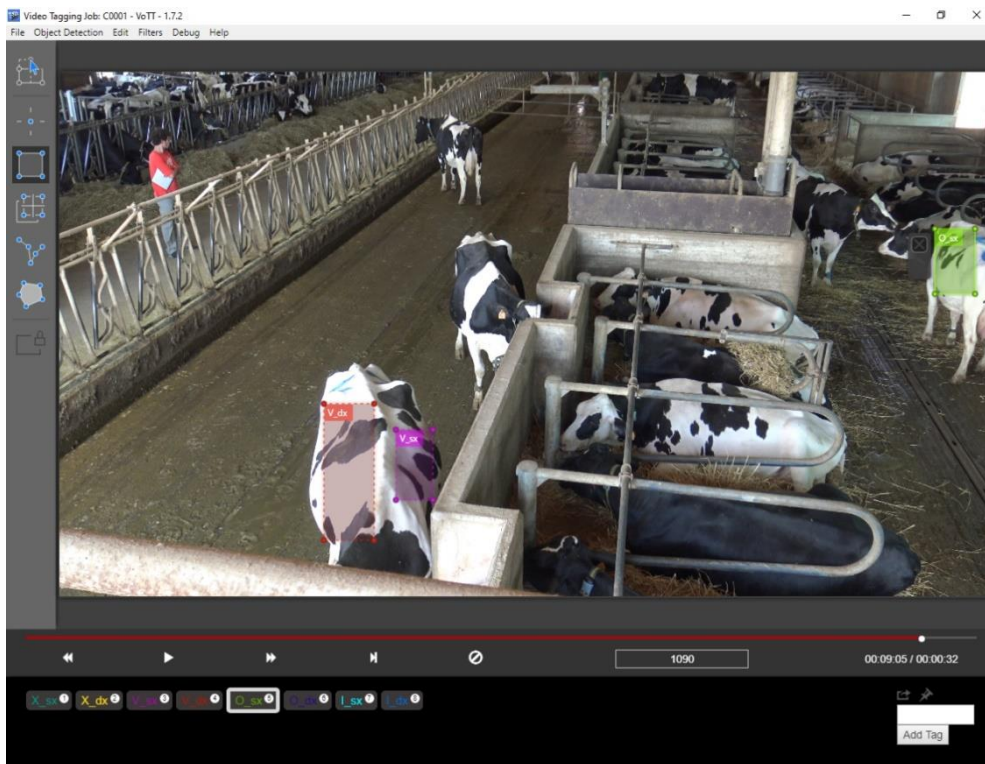
232

233 The videos were recorded on July 2019, collecting a total duration of 210 min to carry out the study. The frame
234 tagging phase was performed through the abovementioned VoTT software, which allowed to sample the
235 videos at a chosen frequency and to make tags (with bounding boxes) on all the frames. In this study, the
236 sampling frequency for the selection of the frame dataset was chosen equal to 2 frames per second because
237 the scenario does not change in a fast way and so a higher frequency would have been redundant. Therefore,
238 about 25200 frames were sampled. The bounding boxes used for tagging the frames were rectangular, rather
239 than square, because the objects to be tagged, i.e. the pelt of the cows, had generally different horizontal and
240 vertical dimensions. The coat area selected in the tagging bounding box has been the biggest rectangular area
241 (with horizontal orientation) identifiable with continuity within the image of the hip of the cow.

242 Thus, at the end of the tagging phase we obtained:

- 243 • a collection of graphical files corresponding to every sampled frame
- 244 • for each frame, a text data file like the one in Figure 5 containing the class number recognized in the
245 frame (if any), the coordinates of the centroid of the corresponding box and the sizes of the box.

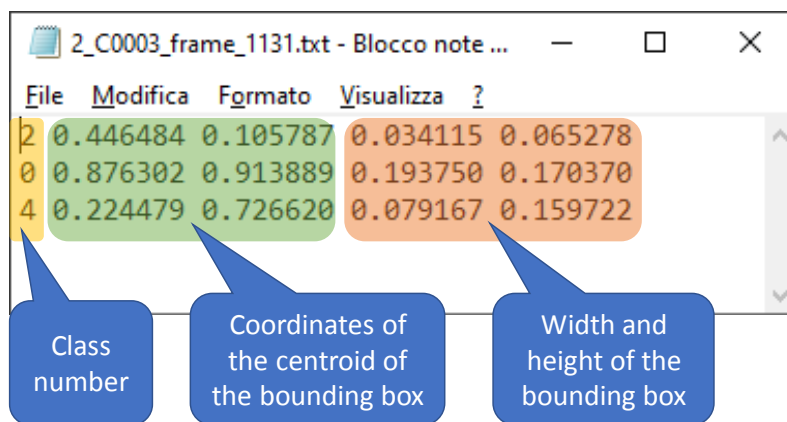
246 A total of 11754 frames showing at least one of the classes were identified and labelled.



247

248

(a)



249

250

(b)

251 Figure 5. Tagging phase through VoTT. (a) Example of graphical file of a frame and (b) example of the data
252 acquired by the tagging process. The coordinates of the centroid and the dimensions of the box are expressed
253 as ratios of the dimensions of the frame.

254

255 The data acquired through the tagging phase were then analyzed to quantify the occurrences of the various
256 target classes. Moreover, the sizes (i.e. width and height) of the bounding boxes were computed as an
257 indicator of the visibility of the target cow within the frame. In fact, a small box may indicate either a position
258 of the cow far from the recording viewpoint, or a partial coverage of the animal by an object in the foreground.

259 The data about the occurrences of the target classes were considered for a proper definition of the split of the
 260 dataset in a training set and a validation set. The criterion adopted for the split was the selection of sets of
 261 consecutives frames accounting for about 80% of the occurrences for each class in the training set and the
 262 remaining 20% for the validation set. 10105 frames for training, 1649 frames for validation. The data resulting
 263 for each class are summarized in Table 1.

264
 265 Table 1
 266 Data resulting from the analysis of the tagging process.

Class code	Class #	Occurrences in the whole dataset
X_{left}	0	1649
X_{right}	1	1575
V_{left}	2	3249
V_{right}	3	839
O_{left}	4	1113
O_{right}	5	649
I_{left}	6	2524
I_{right}	7	771

267
 268 The training and validation of the network was performed by a Nvidia GTX GeoForce 12GB Titan GPU. The
 269 already trained weights downloaded from the Darknet repository (Redmon and Farhadi, 2018) were used as
 270 initial weights for training and 10 000 iterations were performed to obtain the final (adjusted) weights.

271
 272 **2.6 Results assessment**

273 In this subsection the metrics adopted for the evaluation of the performance of the system are presented.
 274 The first metric to introduce is the intersection-over-union (IoU) index, also known as Jaccard index
 275 (Rezatofighi et al., 2019), maybe the most commonly used metric for comparing the similarity between two
 276 general images. IoU encodes the properties of the items under comparison (e.g. widths, heights, locations of
 277 bounding boxes) and then calculates a normalized measure reported in Eq. (1) as the ratio between the area
 278 of the intersection divided by the union of the two bounding boxes (i.e. the predicted and the ground truth
 279 bounding boxes).

280
$$\text{IoU} = \frac{\text{Area of ground truth box} \cap \text{Area of predicted box}}{\text{Area of ground truth box} \cup \text{Area of predicted box}} \quad (1)$$

281 IoU results invariant to the problem scale and thanks to this feature the most of the performance measures in
 282 segmentation, object detection, and tracking are based on this metric (Rezatofighi et al., 2019).
 283 In pattern recognition applications, the precision (P) is the fraction of relevant instances among the retrieved
 284 instances, while the recall (R) is the fraction of relevant instances that have been retrieved over the total
 285 amount of relevant instances. Both precision and recall are therefore based on an understanding and measure
 286 of the relevance. Precision (P) and recall (R) can be expressed, in analytical form, by means of the following
 287 expressions:

$$288 \quad P = \frac{tp}{tp+fp} \quad (2)$$

$$289 \quad R = \frac{tp}{tp+fn} \quad (3)$$

290 Where: tp represents true positive, i.e., the number of cases that the detector successfully detects a class in
 291 an image with IoU greater than a prescribed threshold; fp is false positive, i.e., the number of cases that the
 292 detector reports other objects as a target class in an image, or IoU is less than a prescribed threshold; fn is
 293 false negative, i.e. the number of cases that the detector fails to detect a target class in an image. In the present
 294 work, the specific threshold has been fixed equal to 0.5. Precision is also known as “positive predictive value”,
 295 while recall is also called “true positive rate” or “sensitivity” and this last represents the proportion of actual
 296 positives are correctly identified.

297 In the interpretation of computer vision results, the balanced F_1 -score (also F-score or F-measure) is a metric
 298 that combines both P and R and represent the harmonic mean (Nie et al., 2019):

$$299 \quad F_1 = 2 \cdot \frac{P \cdot R}{P+R} = \left(\frac{P^{-1}+R^{-1}}{2} \right)^{-1} \quad (4)$$

300 This metric coincides with the square of the geometric mean divided by the arithmetic mean of precision and
 301 recall and is clearly close to the arithmetic mean of the two when P and R have similar values. F_1 reaches its
 302 best value at 1.0 and the worst at 0.0.

303 Moreover, the confidence score C (%) has been considered, which quantifies the reliability of the recognition
 304 of a given object within a frame. Confidence score can be calculated using the formula:

$$305 \quad C = Pr \times IoU \quad (5)$$

306 where: Pr represents the detection probability assessed by the network that the object at hand belongs to the
 307 class attributed to it.

308 Precision and recall have been computed for each class based on different confidence thresholds ranging from
 309 0 to 100%, and the precision-recall curves have been drawn for each class. Besides, AP (average precision) is
 310 a popular metric measuring the accuracy of object detectors. AP computes the average precision value for
 311 recall value from 0 to 1 for a specific class (Szeliski, 2011). Therefore, AP can be computed as the area under
 312 the P-R curve of such class. Then, the mean average precision (mAP) of the network was assessed as the mean
 313 of the AP values of the different classes. With analogous criteria is possible to define the average IoU (AIoU)
 314 for a specific class as the average of all the IoU values of the occurrences of the same class.

315

316 3. Results and Discussion

317 3.1 *With original data frames*

318 This subsection deals with the main results obtained by considering the original set of frames described in the
 319 previous section. The set is constituted by 11754 frames, 10105 (about 85% of the total dataset) have been
 320 used for the network training whereas 1649 (about 15%) for the network validation test. The frames to be
 321 used in the validation phase were carefully selected in order to guarantee that all the 8 considered classes
 322 were adequately represented in the frames. The occurrences of each class are reported in Table 2, for both
 323 training and validation phases. Obviously, the sum of the occurrences of all the classes, i.e. 10167 and 2202
 324 respectively for training and validation phases, are bigger than the total frame number since some frames
 325 includes multiple cows belonging to different classes.

326

327 Table 2

328 Number of occurrences and average area of the bounding box for each class and for both training and
 329 validation original datasets.

Training dataset									
	X_{left}	X_{right}	V_{left}	V_{right}	O_{left}	O_{right}	I_{left}	I_{right}	Sum
O_t	1325	1273	2599	673	904	512	2270	611	10167
A_t	0.01063	0.00920	0.00540	0.01688	0.00538	0.01567	0.00447	0.00502	-
$O_t \times A_t$	14.08	11.71	14.03	11.36	4.86	8.02	10.15	3.07	-
Validation dataset									

	X_{left}	X_{right}	V_{left}	V_{right}	O_{left}	O_{right}	I_{left}	I_{right}	Sum
O_v	324	302	650	166	209	137	254	160	2202
A_v	0.02748	0.01540	0.00356	0.01306	0.01542	0.01364	0.01552	0.01275	-
$O_v \times A_v$	8.90	4.65	2.31	2.17	3.22	1.87	3.94	2.04	-

330

331 The validation of the computer vision detection could be carry out from a visual (or graphical) point of view,
 332 by looking if in one specific frame the classes object of the test (in this case the 8 hips of the 4 cows) are
 333 properly identified by the neural network. For example, Figure 6 shows in the yellow box, in the magenta box
 334 and in the green box, the identification of the left hip respectively of the cow O, cow X and cow V. The accuracy
 335 of the detection, reported in the rectangle at top-right of the figure, represent the confidence score C for each
 336 class, as calculated by YOLO, and could be correlated to the probability of finding the cow in the bounding box.
 337 For the frame in the Figure 6, for example, the detection results very good since the class O_{left} and V_{left} have C
 338 of 100% whereas X_{left} has C about 98%.



339

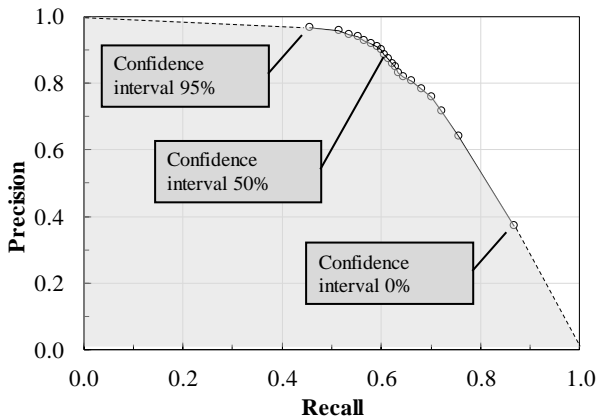
340 Figure 6. Example of visual validation of the classes in a frame. The yellow box (O_{sx}) is the identified left hip
 341 of the cow marked with the letter O; the magenta box (X_{sx}) is the identified left hip of the cow X and the
 342 green box (V_{sx}) is the identified left hip of cow V.

343

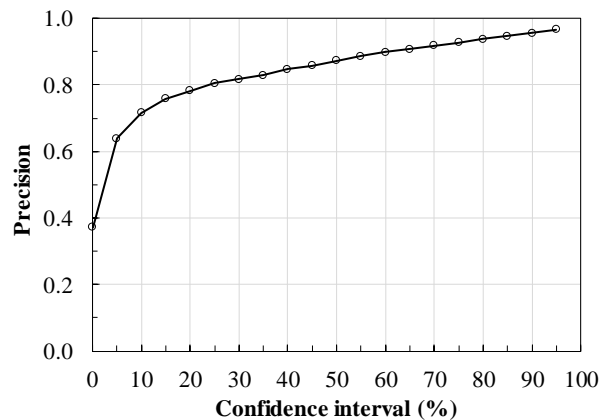
344 In addition, the validation of the neural network can be performed from a mathematical point of view on the
 345 basis of global P and R scores (i.e. considering the whole data set coming from the various classes). As an

346 example, Figure 7(a) shows the global P-R graph (i.e. considering the dataset of the all 8 classes considered in
 347 the study) of the validation test. The trend of the global P-R graph was obtained by considering 20 different
 348 confidence interval (CI) with increasing confidence level, from 0.0% to 95% with step 5%, for the assessment
 349 of the detections based on the IoU of the single detection. As a general trend, the lower confidence interval
 350 produces points with low P and high R values. The opposite for high confidence interval. It seems useful to
 351 remember that the optimal graph trend should be that presenting high level of precision (i.e. higher than 0.8)
 352 all along the R value. Figures 7(b) and 7(c) respectively show the trend of P and R for the different CI values.
 353 For the case at hand the P value is adequate (i.e. higher than 0.8) for CI higher than 20%. For CI equal to 20%
 354 the R value is about 0.7 and it means the neural network is able to detect about the 70% of the “real”
 355 occurrences of the different classes for the various frames. Table 3 reports the main data resulting from the
 356 validation phase and related to the whole dataset. Moreover, same table reports the global F_1 -score and IoU
 357 values for each CI, also depicted in Figure 7d. IoU values go from 0.75 to 0.81 with an AIOU equal to 0.78. In
 358 the object detection field values higher than 0.7 until 1.0, commonly, identified detections good to excellent,
 359 then we reached, on average, a rather good detection from the network.

360

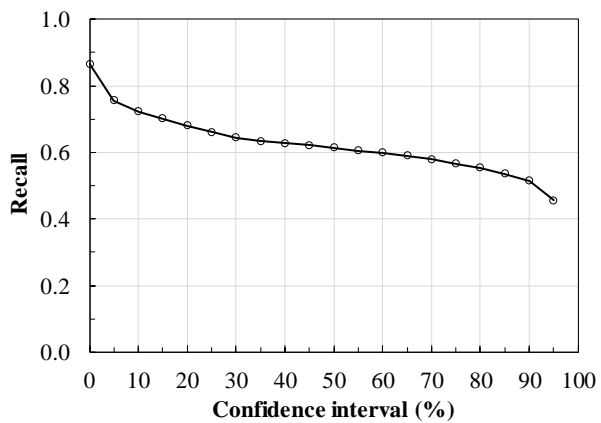


(a)

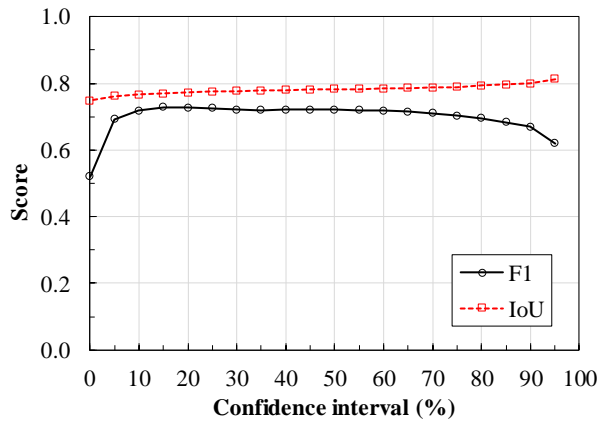


(b)

361
362



(c)



(d)

363
364
365
366
367
368

Figure 7. Principal trends obtained from the validation test by considering all the occurrences dataset and reported for different confidence interval (with original data frames). (a) P-R curve. (b) P trend; (c) R trend; (d) F_1 and IoU score for different confidence interval.

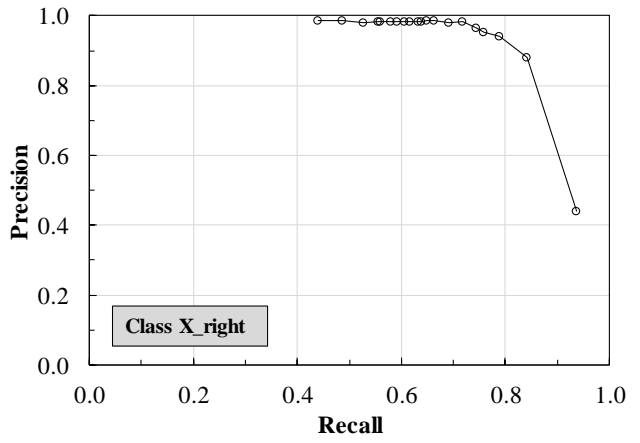
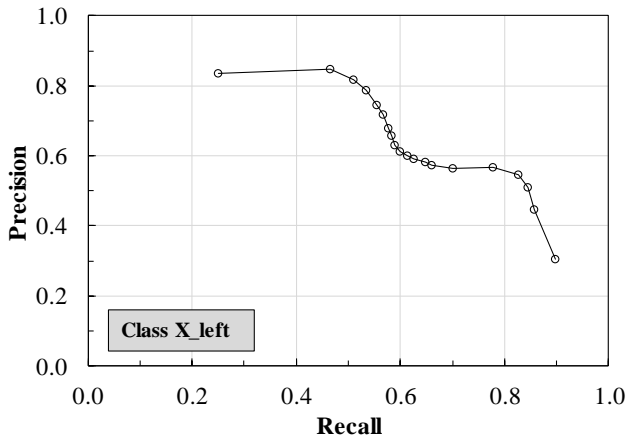
369 Table 3
 370 Main results from the validation test by considering all the occurrences dataset and reported for different
 371 confidence interval (with original data frames).

Confidence interval	True positive*	Ground truth**	Precision	Recall	F ₁ -score	IoU
0.95	1004	1039	0.9663	0.4559	0.6196	0.8126
0.90	1134	1186	0.9562	0.5150	0.6694	0.8000
0.85	1178	1245	0.9462	0.5350	0.6835	0.7960
0.80	1218	1299	0.9376	0.5531	0.6958	0.7928
0.75	1247	1346	0.9264	0.5658	0.7026	0.7891
0.70	1277	1390	0.9187	0.5795	0.7107	0.7874
0.65	1301	1434	0.9073	0.5904	0.7153	0.7853
0.60	1319	1467	0.8991	0.5985	0.7187	0.7838
0.55	1333	1505	0.8857	0.6049	0.7189	0.7833
0.50	1353	1551	0.8723	0.6140	0.7207	0.7821
0.45	1370	1596	0.8584	0.6217	0.7211	0.7811
0.40	1382	1631	0.8473	0.6272	0.7208	0.7803
0.35	1398	1686	0.8292	0.6344	0.7188	0.7790
0.30	1422	1740	0.8172	0.6449	0.7209	0.7774
0.25	1458	1812	0.8046	0.6612	0.7259	0.7752
0.20	1500	1918	0.7821	0.6803	0.7276	0.7723
0.15	1548	2040	0.7588	0.7012	0.7289	0.7700
0.10	1598	2234	0.7153	0.7221	0.7187	0.7665
0.05	1681	2632	0.6387	0.7566	0.6926	0.7617
0.00	2011	5409	0.3718	0.8665	0.5203	0.7480

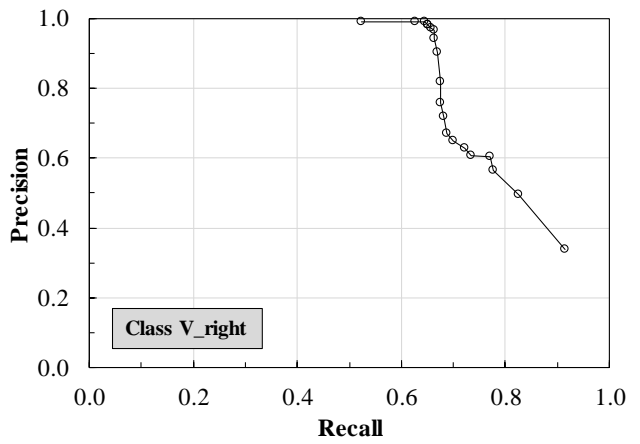
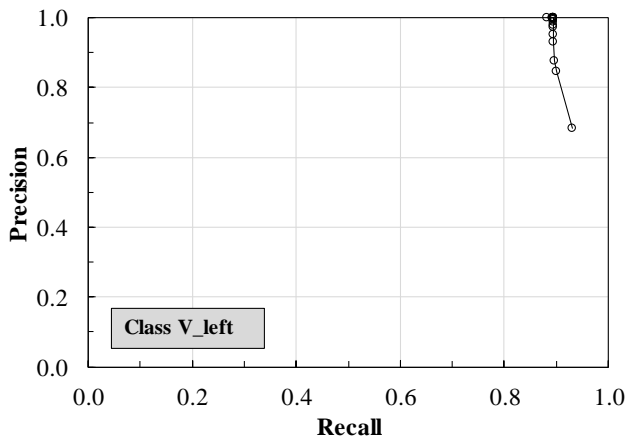
372 * : is the number of true positive occurrences detected from the neural network
 373 ** : is the number of “real” occurrences in the dataset as resulting from the visual detection performed
 374 by the operator.
 375

376 As far as the single class is concerned, Figure 8 shows the Precision-Recall graphs for every considered class
 377 and in Table 4 the most important parameters are collected, useful to judge the detection quality of each
 378 single class. In fact, if in some contexts an “on-average” detection score is sufficient (Szeliski, 2011). In the
 379 present applications, it is not enough being the single class detection score, important as much the “on-
 380 average” score for practical PLF purposes. Then, it is possible to identify in Figure 8, and evaluate from Table
 381 4, the classes with better/worse detection scores. E.g., from the table, the classes with better AP are V_{left} , X_{right}
 382 and O_{left} . Instead, the classes with the worst AP are O_{right} , I_{right} and I_{left} .

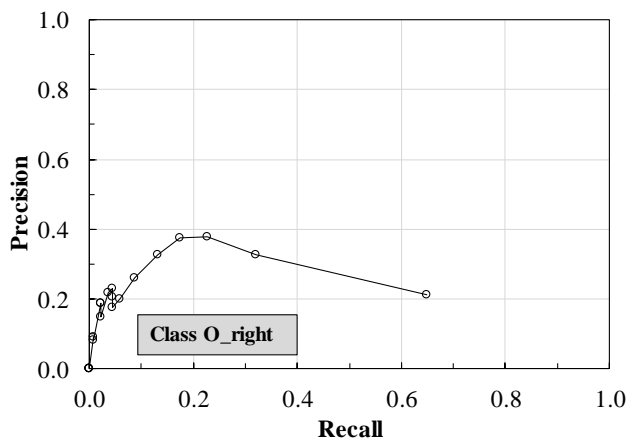
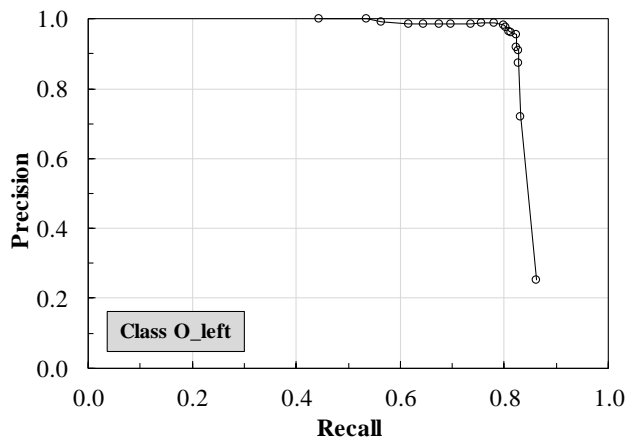
383



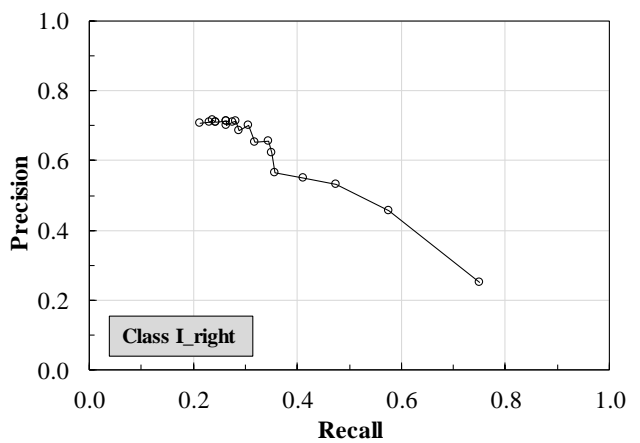
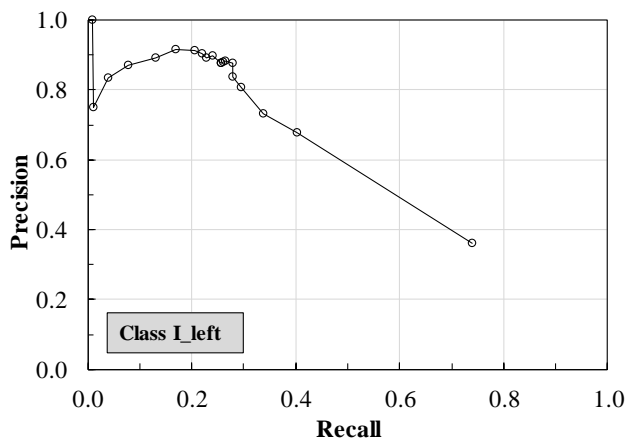
384



385



386



387

388

389

Figure 8. Precision-Recall diagram of the computer vision detection for each one of the 8 target classes by using the original data frames.

390 Even if the AP of the total dataset is 0.7356, some classes have AP value also rather small (i.e. O_{right} , I_{right} and
391 I_{left} with AP values respectively of 0.17, 0.40 and 0.45). The low values for the three worst classes are confirmed
392 by the unusual trends in Figure 8. This analysis should drive the future investigations, oriented them to define
393 the main causes of the low scores and to look for the adequate corrective actions. Differently from the previous
394 discussed scores, the AIoU values are quite similar for the various classes are the AIoU-based identification of
395 the worst classes is more difficult. This confirms some well-known weaknesses and limitations of this metric
396 (Szeliski, 2011) useful to decide, with regards to an object, whether a prediction is correct or not, but it is not
397 suitable to describe the precision of the prediction. For the sake of completeness, the conducted validation
398 test provides a value of $mAP=0.6350$ obtained as mean value among the 8 classes.

399 Finally, in order to establish possible correlations between the main features of the dataset and the outcomes
400 from the validation test, the correlation matrix, reported in Figure 9, has been realized and adopted for the
401 evaluation. Six independent variables, numerically quantifiable, have been selected (i.e. Occurrences, Average
402 Area of the bounding boxes and the product Occurrences \times Average Area of the bounding boxes for both
403 training and validation datasets). Two dependent variables have been selected among the metrics adopted to
404 evaluate the reliability of the detections (i.e. AP and AIoU).

405 Then the correlation matrix has dimension 8×8 . The numerical values adopted for the creation of the
406 correlation matrix are those reported in Table 2 and Table 4.

407 Table 4

408 Summary of the results from the validation test for each class by considering the original data frames.

	X_{left}	X_{right}	V_{left}	V_{right}	O_{left}	O_{right}	I_{left}	I_{right}	Total
AP	0.6485	0.8627	0.9202	0.7838	0.8336	0.1698	0.4583	0.4027	0.7356
AIoU	0.6625	0.7600	0.8547	0.7691	0.7553	0.5232	0.6999	0.7333	0.7812

409

410 The main aspects are the following:

- 411 • (see column #1, row #4,) the occurrences of the different classes populating training and validation
412 datasets, shows good correlations confirming a proper subdivision of the frames into the training group
413 and validation group (the slope of the linear regression represent the ratio $20\%/80\%=0.25$ of used for the
414 subdivision of the whole frame dataset);

- 415 • (see column #1, rows #7, #8 and #9) a characteristic trend exists between number of occurrences in the
 416 training dataset and the metrics used for the evaluation of the detection quality (i.e. AP and AIoU). By
 417 increasing the number of occurrences until a certain “threshold” value it increases in a considerable way
 418 the metric values, but after this threshold, the trend (see dashed red line in the subfigures) presents a
 419 knee characterized by a second branch with low slope. Then, it is like to say that after certain threshold
 420 (occurrences) value a considerable augment of the number of occurrences produces almost negligible
 421 improvement in the detections;
- 422 • (see column #4, rows #7, #8 and #9) the same evaluation is valid also for the relation between number of
 423 occurrences in the validation dataset and the metrics used for the evaluation of the detection quality;
- 424 • the area of the bounding boxes shows no significant correlation with the metrics of reliability of the
 425 detections (see columns #2 and #5). Nevertheless, the features obtained by the product “Occurrences ×
 426 Average Area of the bounding boxes” (see columns #3 and #6) shows a positive correlation with the
 427 metrics, although it is not possible to identify a clear regression curve. However, if we exclude the two
 428 classes with values of the product $O_t \times A_t$ of the training phase significantly smaller than all the other
 429 classes, i.e. O_{left} and I_{right} , a quadratic regression curve of the relationship between AP and $O_t \times A_t$ is
 430 recognizable, with $R^2=0.837$ and the following equation:

431
$$y = -0.0272 x^2 + 0.7111 x - 3.8179 \quad (6)$$

432 This indicates that for the classes having $O_t \times A_t > 8$, AP rapidly increases up to $O_t \times A_t$ near to 12, then it
 433 becomes almost constant. This result shows that is possible to identify optimal values for the occurrence
 434 number and the bounding box areas in the training phase, which could be very useful to efficiently plan
 435 video acquisition to use for train the deep learning network. Therefore, this aspect deserves further and
 436 more in-depth investigations that will be carried out in future experimental campaigns carried out with
 437 additional video shooting.

- 438 • lastly (see columns #7, row #8) a positive correlation is confirmed between AP and AIoU.

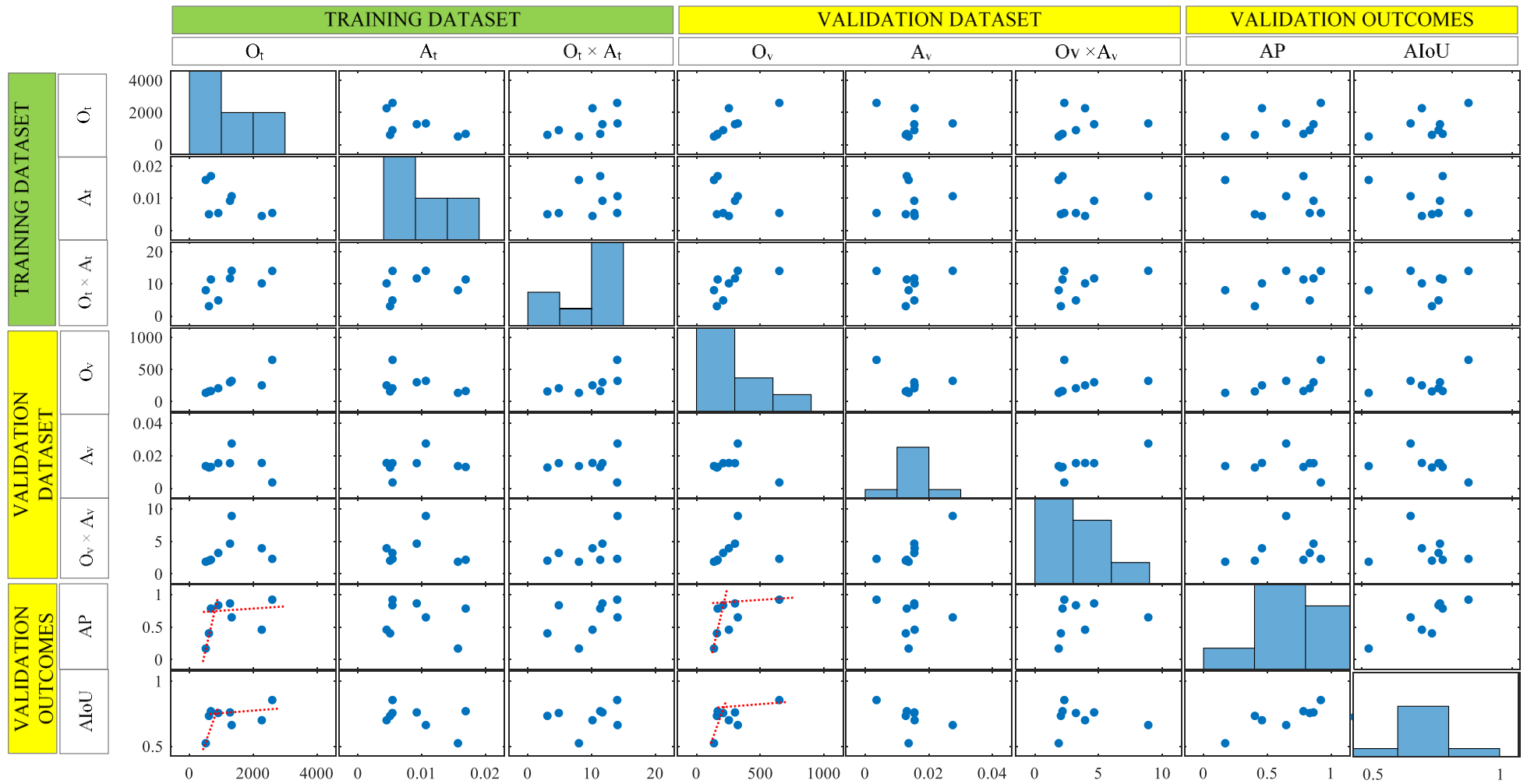
439 These results provide useful indications for both the selection of the strategies more convenient in order to
440 improve the detection quality and the development of optimal datasets for the application investigated in this
441 paper.

442 First of all, if some classes are detected with poor precision, increasing the occurrences in the training dataset
443 the detection accuracy is expected to rise. It makes no sense to increase the occurrences of all classes,
444 especially for those classes that already have suitable metric values, because this would increase the costs of
445 the labelling phase and the computational time of the training phase without producing considerable
446 improvements.

447 Above a certain threshold value of the metrics, it also seems that increasing even the occurrences of the
448 training dataset does not produce considerable benefits. So in such cases, probably alternative solutions are
449 to be sought, such as the replacement of some data frames with others more informative for the network.

450 Finally, it seems that the average area of bounding boxes used for animal detection is not so influential, while
451 the product of number of occurrences and box area is positively correlated with the average precision. This
452 from a practical point of view has considerable advantages for the type of application investigated here, since
453 typically in facilities such as cattle barns the videos are taken from considerable distance (even several tens of
454 meters) due to logistical and security reasons of the cameras. On the other hand, the possibility to record
455 videos from far away means that few cameras could be sufficient to cover large areas typical of cattle farms.

456 The evaluation and the development of these further steps in the process of developing the applications of
457 computer vision systems to the dairy cow sector will be the first objectives of future research work.



458

459 Figure 9. Correlation matrix between some features of the training dataset (i.e. O_t , A_t and $O_t \times A_t$) and validation dataset (i.e. O_v , A_v and $O_v \times A_v$) selected as
 460 independent variables and some metric outcomes of the validation phase selected as dependent variables.

461

462 3.2 *With augmented data frames*

463 This subsection presents a first preliminary attempt to increase the detection quality of some classes. In this
464 case, the four classes with lowest total occurrence number (i.e. V_{right} , O_{left} , O_{right} and I_{right}) have been selected
465 and by adopting a procedure of data augmentation, their total occurrence number have been increased. The
466 two main objectives of the data augmentation test were:

- 467 i) to understand if simple alteration of the original frames can constitute a viable method to increase the
468 available frame datasets in the context of cow detection and, following authors' knowledge, this represent
469 the first application of this type of methods in the herd monitoring research field;
- 470 ii) to estimate the improvement of the detection performances of the network, in terms of AP, connected to
471 the augment of the number of occurrences.

472 In order to judge the possible relation between augment of the number of occurrences and AP improvement,
473 different threshold values have been investigated for the four classes. The following parameter Δ_o (%) has
474 been adopted for the identification of the augment of the number of occurrences:

$$475 \Delta_o (\%) = \text{Augment}_t / O_t \times 100 \quad (7)$$

476 where: Augment_t is the increase of the occurrence number respect to the original dataset in the frames
477 used for the training; O_t is the occurrence number in the frames of the original dataset used in the training.

478 Four different target ranges have been considered for Δ_o (three below 50%, i.e. 10-20%; 20-30%; 30-40% to
479 test the low rates of increase and one above, i.e. 60-80%) and every class has been associated to one of the
480 ranges in order to increase the number of occurrences of the different classes in different ways. In this way
481 has been possible to estimate a correlation between increase of occurrences and increase of detection
482 performances when artificial frames are added in the dataset.

483 The data augmentation procedure has selected some frames, randomly extracted among those containing the
484 four classes indicated above, and artificially have produced a modified copy of every selected frames. The
485 modified copy has been obtained by changing the brightness level of the original frame so simulating possible
486 different light conditions. This procedure, performed with the software XnConvert (Allan et al., 2019), creates
487 a series of modified frames that could really occur in the stable. As an example, Figure 10 shows the

488 comparison between the original and modified frame created by means of the described procedure. The 919
489 modified frames have been added to the original dataset (with 10105 frames) in order to constitute the
490 augmented dataset (with 11024 frames in total).

491



(a)

(b)

492
493
494 Figure 10. Comparison between (a) the original frame as recorded and (b) the modified frame created
495 modifying the brightness of the image.

496

497 Also in this case the frames to be used in the validation phase were carefully selected in order to guarantee
498 that all the 8 considered classes were adequately represented in the frames. The occurrences of each class, in
499 the augmented dataset have been reported in Table 5, for both training and validation phases. The table also
500 collects the augment of the occurrences, for each class, with respect to the original dataset. The augment of
501 occurrences have generated Δ_0 values equal to 29.0%, 15.9%, 71.3% and 37.5% for V_{right} , O_{left} , O_{right} and I_{right}
502 respectively. In total, the augments of occurrences have been 1048, 158 and 1206 respectively for training,
503 validation and total datasets. It is worth to highlight that original dataset, in terms of occurrences, has been
504 augmented of about 10%, with the major increases related to training dataset of the classes V_{right} , O_{left} , O_{right}
505 and I_{right} .

506

507 Table 5

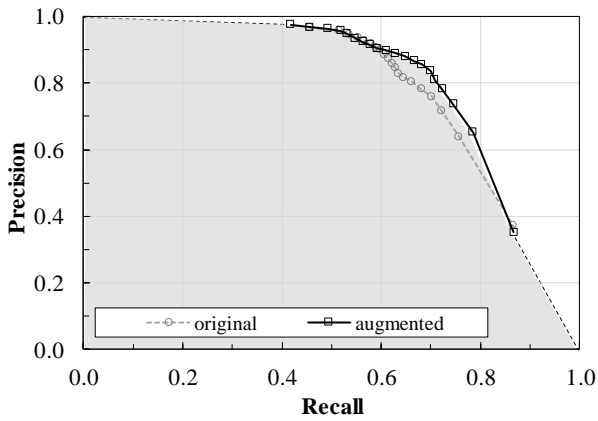
508 Number of occurrences for each class for both training and validation augmented datasets. Augment is the
509 increase on the occurrence number respect to the original datasets.

Training dataset									
	X _{left}	X _{right}	V _{left}	V _{right}	O _{left}	O _{right}	I _{left}	I _{right}	Sum
O _t	1383	1384	2668	868	1048	877	2147	840	11215
Augment _t	58	111	69	195	144	365	-123	229	1048
Validation dataset									
	X _{left}	X _{right}	V _{left}	V _{right}	O _{left}	O _{right}	I _{left}	I _{right}	Sum
O _v	331	302	656	176	218	139	377	161	2360
Augment _v	7	0	6	10	9	2	123	1	158

510

511 Then, the process follows the same steps used for the analysis on the original dataset, and for the sake of
512 comparison with the previous case, analogous graphs and tables are reported in the following in order to
513 summarize the main results. Figure 11(a) reports the global P-R graphs of the validation test obtained for both
514 original and augmented datasets by considering all the 8 classes. From the comparison between the two
515 curves it emerges that also the introduction of very similar frames, which differ only in brightness from the
516 original, can improve both the precision (P) and the network's detection quality. In fact, for the present
517 dataset, the precision improves in the CI range from 10% to 50% (see Figure 11(b)). Conversely, the recall (R)
518 has an anti-symmetric trend with respect to CI of 50%. It improves in the CI from 0% to 50% and slightly
519 deteriorates for CI higher than 50% (see Figure 11(c)). Same trend is obtained for the F₁-score (see Figure
520 11(d)). As far as the IoU metrics is concerned, it decreases about 8-9% all along the CI set. For the case at hand,
521 the P value is adequate (i.e. higher than 0.8) for CI higher than 15%. For CI equal to 15% the R value is about
522 0.75. Table 6 collects all the results graphically reported in Figure 11.

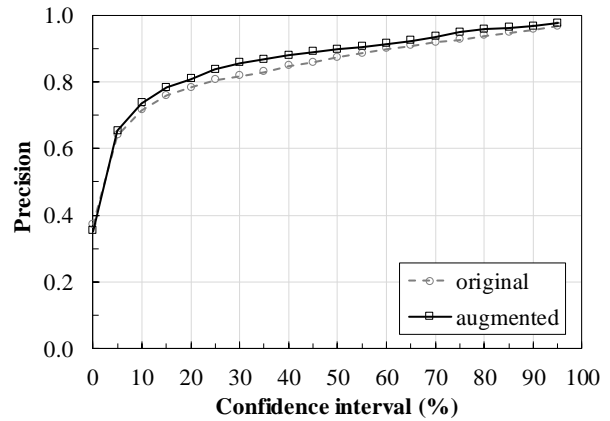
523



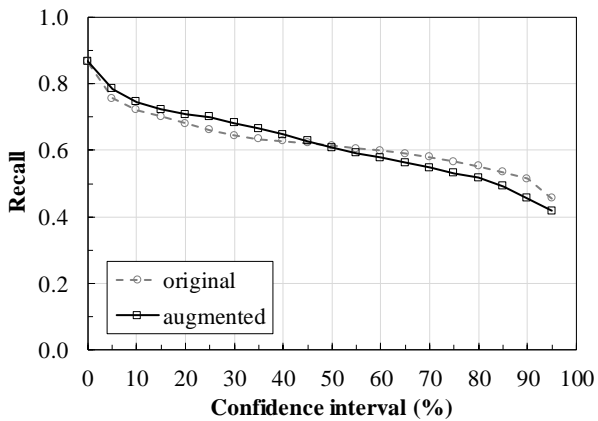
524

525

(a)



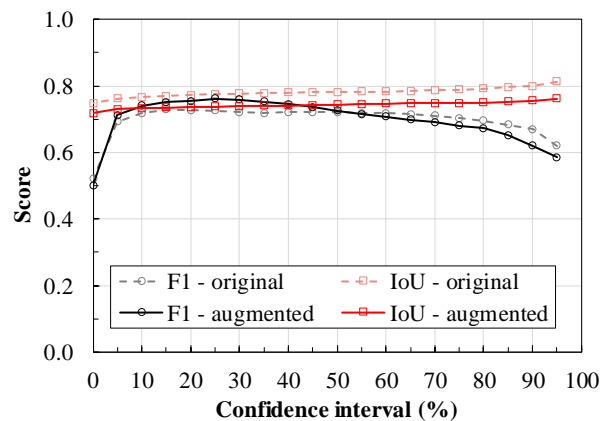
(b)



526

527

(c)



(d)

528 Figure 11. Comparison between the principal trends obtained from the validation test by considering all the
 529 occurrences dataset and reported for different confidence interval (with both original and augmented data
 530 frames). (a) P-R curve. (b) P trend; (c) R trend; (d) F_1 and IoU score for different confidence interval.

531

532 As far as the single class is concerned, in Table 7 are collected the parameters used to judge the detection
 533 quality of the various classes and Figure 12 shows the Precision-Recall graphs of each single class. From the
 534 table, the classes with better AP are V_{left} , O_{left} and V_{right} . Instead, the classes with the worst AP are O_{right} , I_{right}
 535 and X_{left} .

536

537 Table 6

538 Main results from the validation test by considering all the occurrences dataset and reported for different
539 confidence interval (with augmented data frames).

Confidence interval	True positive*	Ground truth**	Precision	Recall	F ₁ -score	IoU
0.95	986	1011	0.9753	0.4178	0.5850	0.7615
0.90	1076	1113	0.9668	0.4559	0.6196	0.7563
0.85	1162	1207	0.9627	0.4924	0.6515	0.7533
0.80	1223	1278	0.9570	0.5182	0.6723	0.7506
0.75	1253	1322	0.9478	0.5309	0.6806	0.7489
0.70	1293	1383	0.9349	0.5479	0.6909	0.7484
0.65	1328	1438	0.9235	0.5627	0.6993	0.7477
0.60	1363	1491	0.9142	0.5775	0.7079	0.7463
0.55	1396	1544	0.9041	0.5915	0.7152	0.7454
0.50	1437	1601	0.8976	0.6089	0.7256	0.7439
0.45	1483	1668	0.8891	0.6284	0.7363	0.7424
0.40	1529	1739	0.8792	0.6479	0.7460	0.7410
0.35	1571	1812	0.8670	0.6657	0.7531	0.7403
0.30	1609	1880	0.8559	0.6818	0.7590	0.7392
0.25	1652	1976	0.8360	0.7000	0.7620	0.7377
0.20	1671	2067	0.8084	0.7081	0.7549	0.7371
0.15	1707	2183	0.7820	0.7233	0.7515	0.7351
0.10	1760	2391	0.7361	0.7458	0.7409	0.7329
0.05	1854	2843	0.6521	0.7852	0.7125	0.7296
0.00	2090	5927	0.3526	0.8669	0.5013	0.7184

540 * : is the number of true positive occurrences detected from the neural network

541 ** : is the number of "real" occurrences in the dataset as resulting from the visual detection performed
542 by the operator.

543

544 Table 7

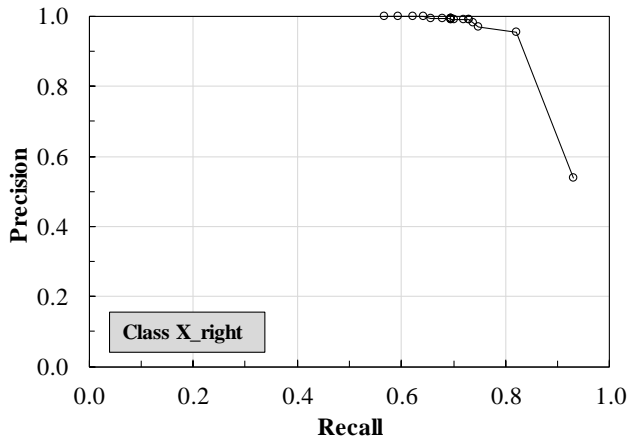
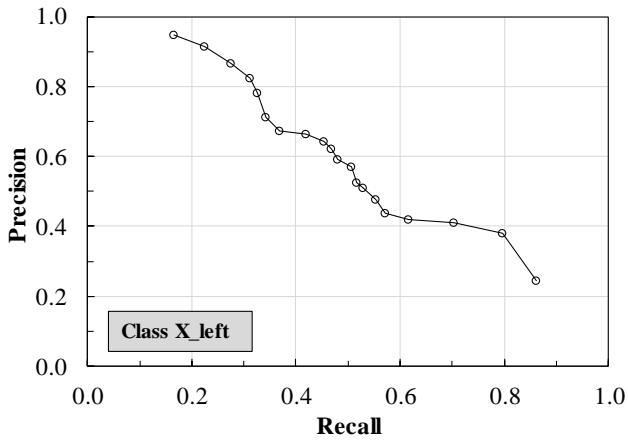
545 Summary of the results from the validation test for each class by considering the augmented data frames.

	X _{left}	X _{right}	V _{left}	V _{right}	O _{left}	O _{right}	I _{left}	I _{right}	Total
AP	0.5489	0.8755	0.9405	0.8815	0.8954	0.2405	0.7618	0.5391	0.7559
AIoU	0.7034	0.7593	0.7481	0.8153	0.7221	0.6392	0.6635	0.7865	0.7428

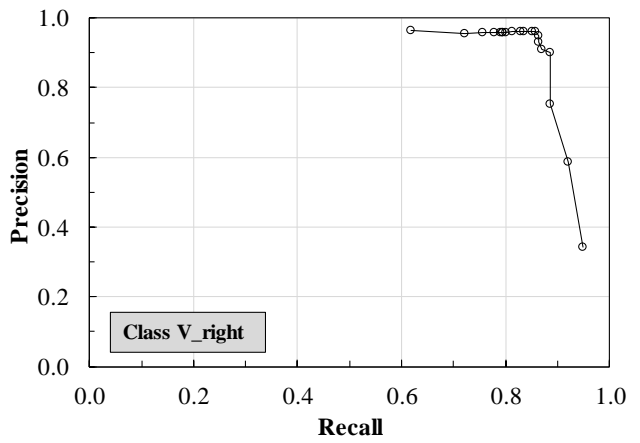
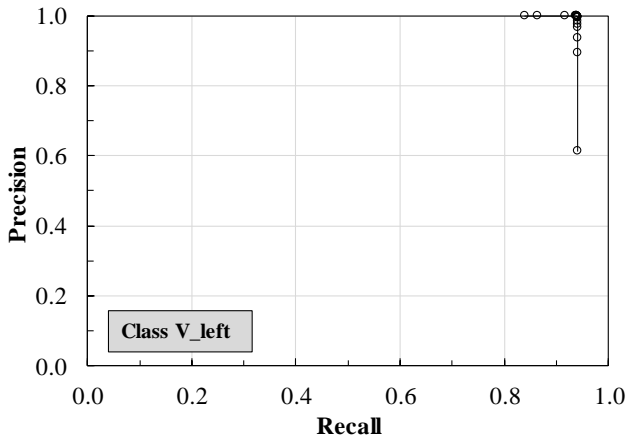
546

547

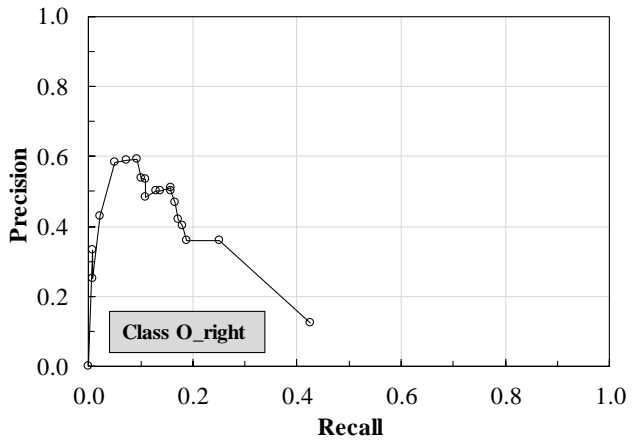
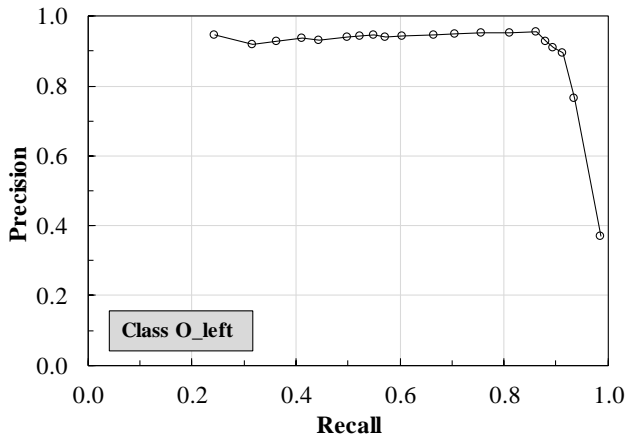
548



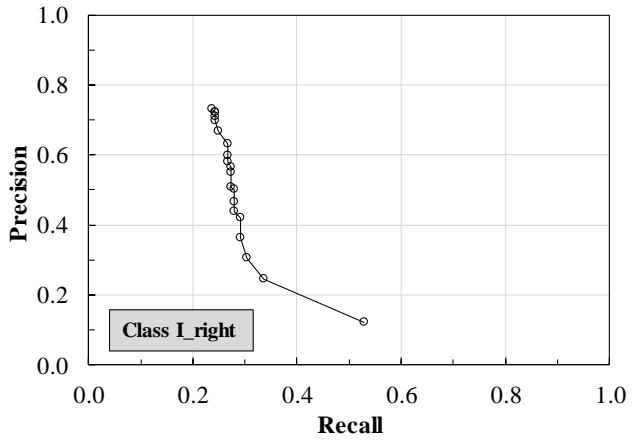
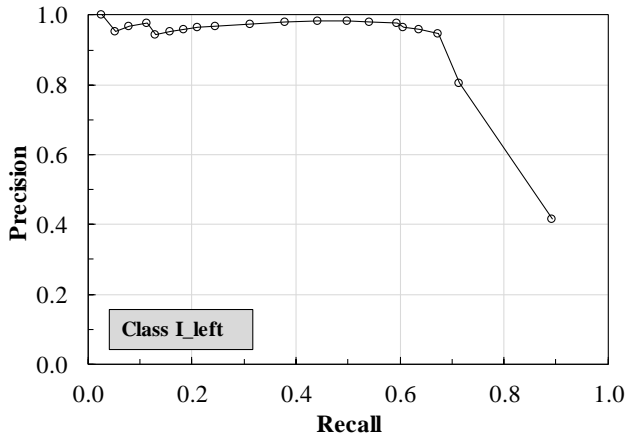
549



550



551



552

553

554

555

Figure 12. Precision-Recall diagram of the computer vision detection for each one of the 8 target classes by using the augmented data frames.

556 In order to compare the network detection performances of the original and augmented data frame cases,
 557 the following parameter Δ_{AP} (%) has been defined and calculated for the four classes majorly influenced by the
 558 data augmentation procedure:

$$559 \quad \Delta_{AP} (\%) = (AP_{\text{augmented}} - AP_{\text{original}}) / AP_{\text{original}} \times 100 \quad (8)$$

560 where: $AP_{\text{augmented}}$ is the average precision obtained using the augmented dataset; AP_{original} is the average
 561 precision obtained using the original dataset.

562 The values of Δ_O and Δ_{AP} , representing a (percentage) relative difference of occurrences and average precision
 563 respectively, are reported in Table 8 for the four classes of interest.

564

565 Table 8

566 Percentage relative difference of occurrences (Δ_O) and average precision (Δ_{AP}) for the four classes mainly
 567 influenced by the data augmentation procedure.

	V_{right}	O_{left}	O_{right}	I_{right}
Δ_O (%)	29.0	15.9	71.3	37.5
Δ_{AP} (%)	12.5	7.4	41.6	33.9

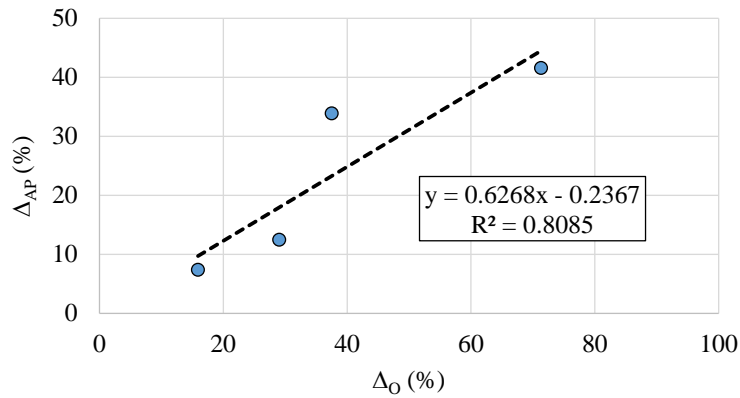
568

569 By the analysis of the Δ_{AP} values in Table 8, it emerges that the augmented dataset is able, in general, to provide
 570 an improvement of the metric values, or i.e. is able to increase also the single class detection quality of the
 571 neural network, especially for those classes characterized by a considerable augment of occurrences. This was
 572 probably expected, but the most important outcomes may be that, also for the single classes, the introduction
 573 of artificially-obtained frames is suitable to increase the detection scores. This aspect has important practical
 574 implications since in applications similar to the one studied here it is not always possible to record videos for
 575 long periods.

576 Figure 13 graphically shows the position of the values of Δ_O and Δ_{AP} reported in Table 8. The further emerging
 577 outcome is that exist a clear direct relation between the increase of the occurrences number and the detection
 578 performances of the network and the relation seems almost linear, at least for the investigated ranges.

579

580



581

582 Figure 13. Percentage relative difference of occurrences (Δ_O) Vs. average precision (Δ_{AP}) for the four classes
 583 mainly influenced by the data augmentation procedure.

584

585 These outcomes confirm that for the situations in which the number of frames is not sufficient to provide a
 586 suitable occurrence number for some classes, in order to increase the detection performance of the network,
 587 a reliable strategy could be augment the dataset by adopting “virtual” frames made in-house and ad-hoc for
 588 the single classes not adequately represented in the acquired videos. This will be object of future investigations
 589 and further details are not reported here since they are beyond the scope of this paper. For the sake of
 590 completeness, the conducted validation test provides a value of mAP=0.6604, higher than the value obtained
 591 for the original dataset.

592 The developed system is suitable to implement various future extensions performing tracking and
 593 identification of anomalous behaviours. Cows tracking can be achieved by the integration of algorithms
 594 capable to compute the IoU between chronologically subsequent frames. IoU rate can be interpreted as
 595 displacement of the animal if it overcomes a predefined threshold. This will allow to record the trajectories of
 596 individual animals and also to compute the time spent in different positions, thus providing an accurate proxy
 597 of the time budget of every cow. Furthermore, this approach can be also used to detect standing time and
 598 lying bouts, which can be used to assess welfare indices of the herd, or different groups or even individual
 599 animals. Moreover, the evaluation of a different detection algorithm will be also object of future investigations.

600

601

602 4. Conclusions

603 This study represents the first step for the development of a detection system aiming to recognize individual
604 cows, evaluate their position, understand the action the cow is carrying out and finally tracking the cow
605 movements in the barn. A computer vision system based on deep learning models for the automatic detection
606 of individual cow based on the pelt pattern, within images using an HD resolution camera, was designed and
607 implemented in a case study barn.

608 The global detection performances of the network, reported in terms of precision-recall curves, have been
609 proved to be good for some classes and excellent for others since the AIoU is about 0.78 and the IoU for the
610 different classes ranges from 0.75 to 0.81. The performances of the network is confirmed by the F_1 -score
611 ranging from 0.67 to 0.73 for common confidence interval from 5% to 90%. The outcomes proved that the
612 natural pattern of the cow pelt investigated in the study is suitable for the animal detection, all this
613 representing a necessary step prior to understand the cow action. Moreover, in this study a useful still simple
614 equation has been proposed for the evaluation of the optimal values for the occurrence number and the
615 bounding box areas in the training phase. The regression procedure for the equation calibration showed that
616 a quadratic relation exists between AP and $O_t \times A_t$. This proposal could be very useful to efficiently plan the
617 acquisition to use for train the network in this type of context. Finally, the application of a very simple data
618 augmentation technique, changing the frame brightness level, has been confirmed to be an effective strategy
619 to adopt in order to improve the performances of the network, in case of insufficient occurrences.

620 The promising results reported here present the first phase of the work for the definition of a computer vision-
621 based system for herd monitoring applications devoted to the study of movements, actions and behavior of
622 the cows in a barn.

623

624 **Acknowledgements**

625 The authors wish to thank Prof. Andrea Formigoni, Scientific Supervisor of the Experimental and Didactic Dairy
626 Cows Unit of the University of Bologna, where all the video recordings, images and data necessary for carrying
627 out the research have been acquired.

628

629 **Funding**

630 The activity presented in the paper is part of the research project PRIN 2017 “Smart dairy farming: innovative
631 solutions to improve herd productivity” funded by the Italian Ministry of Education, University and Research
632 [20178AN8NC].

633

634

635 **References**

- 636 AFIMILK, 2020. Cow monitoring. website. URL <https://www.afimilk.com/cow-monitoring> (accessed
637 5.15.20).
- 638 Allan, E.L., Livermore, L., Price, B.W., Shchedrina, O., Smith, V.S., 2019. A Novel Automated Mass
639 Digitisation Workflow for Natural History Microscope Slides. *Biodivers. data J.* 7, e32342–e32342.
640 <https://doi.org/10.3897/BDJ.7.e32342>
- 641 ALLFLEX, 2020. Herd monitoring. website. URL <https://westgen.com/products/scr-herd-monitoring>
642 (accessed 5.20.20).
- 643 Alsaad, M., Fadul, M., Steiner, A., 2019. Automatic lameness detection in cattle. *Vet. J.*
644 <https://doi.org/10.1016/j.tvjl.2019.01.005>
- 645 Aydin, A., 2017. Development of an early detection system for lameness of broilers using computer vision.
646 *Comput. Electron. Agric.* 136, 140–146. <https://doi.org/10.1016/j.compag.2017.02.019>
- 647 Barkema, H.W., von Keyserlingk, M.A.G., Kastelic, J.P., Lam, T.J.G.M., Luby, C., Roy, J.-P., LeBlanc, S.J., Keefe,
648 G.P., Kelton, D.F., 2015. Invited review: Changes in the dairy industry affecting dairy cattle health and
649 welfare. *J. Dairy Sci.* 98, 7426–7445.
- 650 Berckmans, D., 2014. Precision livestock farming technologies for welfare management in intensive
651 livestock systems. *Rev. sci. tech. Off. int. Epiz* 33, 189–196. <https://doi.org/10.20506/rst.33.1.2273>
- 652 Bewley, J.M., Robertson, L.M., Eckelkamp, E.A., 2017. A 100-Year Review: Lactating dairy cattle housing
653 management. *J. Dairy Sci.* <https://doi.org/10.3168/jds.2017-13251>
- 654 Bezen, R., Edan, Y., Halachmi, I., 2020. Computer vision system for measuring individual cow feed intake
655 using RGB-D camera and deep learning algorithms. *Comput. Electron. Agric.* 172, 105345.
656 <https://doi.org/10.1016/j.compag.2020.105345>
- 657 Cowley, F.C., Barber, D.G., Houlihan, A. V, Poppi, D.P., 2015. Immediate and residual effects of heat stress
658 and restricted intake on milk protein and casein composition and energy metabolism. *J. Dairy Sci.* 98,
659 2356–68. <https://doi.org/10.3168/jds.2014-8442>
- 660 DELAVAL, 2020. Sensors for herd. website. URL <https://www.delaval.com> (accessed 5.12.20).
- 661 Fournel, S., Rousseau, A.N., Laberge, B., 2017. Rethinking environment control strategy of confined animal
662 housing systems through precision livestock farming. *Biosyst. Eng.* 155, 96–123.
663 <https://doi.org/10.1016/j.biosystemseng.2016.12.005>
- 664 Girshick, R., 2015. Fast R-CNN, in: *Proceedings of the IEEE International Conference on Computer Vision*. pp.
665 1440–1448. <https://doi.org/10.1109/ICCV.2015.169>
- 666 Girshick, R., Donahue, J., Darrell, T., Malik, J., 2014. Rich feature hierarchies for accurate object detection
667 and semantic segmentation, in: *Proceedings of the IEEE Computer Society Conference on Computer*
668 *Vision and Pattern Recognition*. pp. 580–587. <https://doi.org/10.1109/CVPR.2014.81>
- 669 Guzhva, O., Ardö, H., Herlin, A., Nilsson, M., Åström, K., Bergsten, C., 2016. Feasibility study for the

670 implementation of an automatic system for the detection of social interactions in the waiting area of
671 automatic milking stations by using a video surveillance system. *Comput. Electron. Agric.* 127, 506–
672 509. <https://doi.org/10.1016/j.compag.2016.07.010>

673 Halachmi, I., Klopčič, M., Polak, P., Roberts, D.J., Bewley, J.M., 2013. Automatic assessment of dairy cattle
674 body condition score using thermal imaging. *Comput. Electron. Agric.* 99, 35–40.
675 <https://doi.org/10.1016/j.compag.2013.08.012>

676 Jaeger, M., Brügemann, K., Brandt, H., König, S., 2019. Associations between precision sensor data with
677 productivity, health and welfare indicator traits in native black and white dual-purpose cattle under
678 grazing conditions. *Appl. Anim. Behav. Sci.* <https://doi.org/10.1016/j.applanim.2019.01.008>

679 Jiang, B., Song, H., He, D., 2019. Lameness detection of dairy cows based on a double normal background
680 statistical model. *Comput. Electron. Agric.* 158, 140–149.
681 <https://doi.org/10.1016/j.compag.2019.01.025>

682 Kamilaris, A., Prenafeta-Boldú, F.X., 2018. Deep learning in agriculture: A survey. *Comput. Electron. Agric.*
683 <https://doi.org/10.1016/j.compag.2018.02.016>

684 Li, W., Ji, Z., Wang, L., Sun, C., Yang, X., 2017. Automatic individual identification of Holstein dairy cows
685 using tailhead images. *Comput. Electron. Agric.* 142, 622–631.
686 <https://doi.org/10.1016/j.compag.2017.10.029>

687 Martinez-Ortiz, C.A., Everson, R.M., Mottram, T., 2013. Video tracking of dairy cows for assessing mobility
688 scores, in: *Joint European Conference on Precision Livestock Farming*,. 10 – 12 September 2013,
689 Leuven, Belgium, p. 8.

690 Microsoft, 2018. VoTT: Visual Object Tagging Tool. GitHub Repos.

691 Nie, X., Yang, M., Liu, R.W., 2019. Deep Neural Network-Based Robust Ship Detection Under Different
692 Weather Conditions, in: *2019 IEEE Intelligent Transportation Systems Conference (ITSC)*. pp. 47–52.
693 <https://doi.org/10.1109/ITSC.2019.8917475>

694 Norouzzadeh, M.S., Nguyen, A., Kosmala, M., Swanson, A., Palmer, M., Packer, C., Clune, J., 2017.
695 Automatically identifying, counting, and describing wild animals in camera-trap images with deep
696 learning, in: *Proceedings of the National Academy of Sciences of the United States of America*. pp. 1–
697 17. <https://doi.org/10.1073/pnas.1719367115>

698 Okura, F., Ikuma, S., Makihara, Y., Muramatsu, D., Nakada, K., Yagi, Y., 2019. RGB-D video-based individual
699 identification of dairy cows using gait and texture analyses. *Comput. Electron. Agric.* 165, 104944.
700 <https://doi.org/10.1016/j.compag.2019.104944>

701 Porto, S.M.C., Arcidiacono, C., Anguzza, U., Cascone, G., 2015. The automatic detection of dairy cow feeding
702 and standing behaviours in free-stall barns by a computer vision-based system. *Biosyst. Eng.* 133, 46–
703 55. <https://doi.org/10.1016/j.biosystemseng.2015.02.012>

704 Porto, S.M.C., Arcidiacono, C., Anguzza, U., Cascone, G., 2013. A computer vision-based system for the

705 automatic detection of lying behaviour of dairy cows in free-stall barns. *Biosyst. Eng.* 115, 184–194.
706 <https://doi.org/10.1016/j.biosystemseng.2013.03.002>

707 Redmon, J., 2013. 2016. Darknet: Open Source Neural Networks in C [WWW Document]. website. URL
708 <https://pjreddie.com/darknet/> (accessed 5.10.20).

709 Redmon, J., Divvala, S., Girshick, R., Farhadi, A., 2016. You only look once: Unified, real-time object
710 detection, in: *Proceedings of the IEEE Computer Society Conference on Computer Vision and Pattern*
711 *Recognition*. IEEE, pp. 779–788. <https://doi.org/10.1109/CVPR.2016.91>

712 Redmon, J., Farhadi, A., 2018. YOLOv3: An Incremental Improvement. *arXiv Prepr.* 1804.02767.

713 Ren, S., He, K., Girshick, R., Sun, J., 2017. Faster R-CNN: Towards Real-Time Object Detection with Region
714 Proposal Networks. *IEEE Trans. Pattern Anal. Mach. Intell.* 39, 1137–1149.
715 <https://doi.org/10.1109/TPAMI.2016.2577031>

716 Rezatofighi, H., Tsoi, N., Gwak, J., Sadeghian, A., Reid, I., Savarese, S., 2019. Generalized intersection over
717 union: A metric and a loss for bounding box regression. *Proc. IEEE Comput. Soc. Conf. Comput. Vis.*
718 *Pattern Recognit.* 2019-June, 658–666. <https://doi.org/10.1109/CVPR.2019.00075>

719 Song, X., Leroy, T., Vranken, E., Maertens, W., Sonck, B., Berckmans, D., 2008. Automatic detection of
720 lameness in dairy cattle-Vision-based trackway analysis in cow's locomotion. *Comput. Electron. Agric.*
721 64, 39–44. <https://doi.org/10.1016/j.compag.2008.05.016>

722 Szeliski, R., 2011. *Computer Vision*, I. ed. Springer-Verlag London, London. [https://doi.org/10.1007/978-1-](https://doi.org/10.1007/978-1-84882-935-0)
723 84882-935-0

724 Taigman, Y., Ming, Y., Ranzato, M., Wolf, L., 2014. DeepFace: Closing the Gap to Human-Level Performance
725 in Face Verification, in: *Conference on Computer Vision and Pattern Recognition (CVPR)*.
726 <https://doi.org/10.1109/CVPR.2014.220>

727 Trnovszky, T., Kamencay, P., Orjesek, R., Benco, M., Sykora, P., 2017. Animal recognition system based on
728 convolutional neural network. *Adv. Electr. Electron. Eng.* 15, 517–525.
729 <https://doi.org/10.15598/aelee.v15i3.2202>

730 Tsai, D.M., Huang, C.Y., 2014. A motion and image analysis method for automatic detection of estrus and
731 mating behavior in cattle. *Comput. Electron. Agric.* 104, 25–31.
732 <https://doi.org/10.1016/j.compag.2014.03.003>

733 Tullo, E., Finzi, A., Guarino, M., 2019. Review: Environmental impact of livestock farming and Precision
734 Livestock Farming as a mitigation strategy. *Sci. Total Environ.*
735 <https://doi.org/10.1016/j.scitotenv.2018.10.018>

736 Van Hertem, T., Alchanatis, V., Antler, A., Maltz, E., Halachmi, I., Schlageter-Tello, A., Lokhorst, C., Viazzi, S.,
737 Romanini, C.E.B., Pluk, A., Bahr, C., Berckmans, D., 2013. Comparison of segmentation algorithms for
738 cow contour extraction from natural barn background in side view images. *Comput. Electron. Agric.*
739 91, 65–74. <https://doi.org/10.1016/j.compag.2012.12.003>

740 Van Hertem, T., Schlageter Tello, A., Viazzi, S., Steensels, M., Bahr, C., Romanini, C.E.B., Lokhorst, K., Maltz,
741 E., Halachmi, I., Berckmans, D., 2018. Implementation of an automatic 3D vision monitor for dairy cow
742 locomotion in a commercial farm. *Biosyst. Eng.* <https://doi.org/10.1016/j.biosystemseng.2017.08.011>
743 Van Hertem, T., Steensels, M., Viazzi, S., Romanini, E.C.B., Bahr, C., Berckmans, D., Schlageter Tello, A.,
744 Lokhorst, K., Maltz, E., Halachmi, I., 2014. Improving a computer vision lameness detection system by
745 adding behaviour and performance measures, in: *International Conference of Agricultural*
746 *Engineering*. pp. 1–8.
747 Ventura, B.A., Von Keyserlingk, M.A.G., Wittman, H., Weary, D.M., 2016. What difference does a visit
748 make? Changes in animal welfare perceptions after interested citizens tour a dairy farm. *PLoS One*.
749 <https://doi.org/10.1371/journal.pone.0154733>
750

CRediT author statement

Patrizia Tassinari: Conceptualization, Funding acquisition, Project administration, Resources, Supervision.

Marco Bovo: Conceptualization, Data curation, Formal analysis, Methodology, Validation, Visualization, Writing—original draft, Writing—review & editing.

Stefano Benni: Conceptualization, Formal analysis, Investigation, Methodology, Supervision, Validation, Visualization, Writing—original draft.

Simone Franzoni: Software

Matteo Poggi: Software

Ludovica Maria Eugenia Mammi: Investigation

Stefano Mattoccia: Conceptualization, Software, Validation

Luigi Di Stefano: Conceptualization, Software, Validation

Filippo Bonora: Data curation

Alberto Barbaresi: Visualization, Writing—review & editing

Enrica Santolini: Visualization, Writing—review & editing

Daniele Torreggiani: Conceptualization, Project administration, Resources, Supervision, Writing—review & editing.